Noise-induced memory in extended excitable systems

Dante R. Chialvo, Guillermo A. Cecchi, and Marcelo O. Magnasco
Center for Studies in Physics and Biology, The Rockefeller University, 1230 York Avenue, New York, New York 10021
(Received 23 March 1999; revised manuscript received 13 December 1999)

We describe a form of memory exhibited by extended excitable systems driven by stochastic fluctuations. Under such conditions, the system self-organizes into a state characterized by power-law correlations, thus retaining long-term memory of previous states. The exponents are robust and model independent. We discuss implications of these results for the functioning of cortical neurons as well as for networks of neurons.

PACS number(s): 87.10.+e, 87.19.La

Neurons receive thousands of perturbations affecting the transmembrane voltage at various points of the synaptic membrane. Recent experimental evidence has shown active nonlinearities [1] at the dendrites of cortical neurons, implying that models representing these neurons must have many nonlinear spatial degrees of freedom.

What are the dynamical consequences of these distributed nonlinearities for neuronal function? The answer is not immediately certain. The prevailing view, since the work of Lapicque in 1907 [2], has been that all input regions (i.e., dendrites) are linear, so neurons can be represented as a single compartment. In this view incoming excitations are linearly integrated, and whenever the resulting value exceeds a predefined threshold an action potential is generated. Thus the neuron is considered to have a single nonlinear degree of freedom: the spatial region where the thresholding dynamics takes place.

This paper describes a robust form of noise-induced memory which appears naturally as a direct consequence of including distributed nonlinearities in the formulation of a neuron's input region. Besides having relevance at the neural level, it touches other areas of biology where excitable models have been used, as is the case for models of forest-fire propagation, spreading of epidemics, and noise-induced waves [3]. From the outset, it needs to be noted that the phenomena to be described do not depend on the type of excitable model one uses.

To show the essence of the main point, we adapt the Greenberg-Hastings cellular automata model [4] of excitable media [5]. For the purpose of this paper let us restrict ourselves to the case of a one-dimensional lattice of coupled identical compartments ($n=1,\ldots,N$), with open boundary conditions. Each spatial location is assigned a discrete state S_n^t which can be one of three—quiescent, excited, or refractory—with the dynamics determined by the transition rules: $E\rightarrow R$ (always), $R\rightarrow Q$ (always), $Q\rightarrow E$ (with probability ρ, or if at least one neighbor is in the E state), and $Q\rightarrow Q$ (otherwise). Excitable systems have a refractory period during which no re-excitation is possible; we introduce it by delaying the transition from the R state to the Q state for r time steps. Thus the only two parameters in the system are ρ, which determines the probability that an input to a given site n result into an excitation (i.e., a transition $Q\rightarrow E$); and r determining the time scale of recovery from the excited state. It turns out that the precise value of r is not crucial, but choosing a value of r at least equal to or larger than the value of N eliminates a number of numerical complications [6].

A dendritic region bombarded by many weak synaptic inputs corresponds to a relatively small value for ρ (here 10^{-2}). The typical response of the model under such conditions is illustrated in Fig. 1. One can see that, starting from arbitrary initial conditions, eventually an element is first excited (left arrow in Fig. 1). This initiates a propagated wave front which collides with others initiated in the same way somewhere else in the system. After the completion of the refractory period the process repeats itself, originating another wave front (right side of Fig. 1). An immediately apparent feature is the overall similarity of any two consecutive fronts. The large-scale shape is preserved, despite the fact that each element is being randomly perturbed.

We found that important information can be extracted from an analysis of the dynamics of the first element to be excited in each wave front, denoted as $L(n)$. Figure 2 shows the results of numerical simulations where $L(n)$ of each wave front is plotted as a function of time. Note the tendency of $L(n)$ to remain near the previous leading site, which is especially apparent in the larger systems. To quantify this dynamics, we numerically estimated $\langle |L^t(n)-L^{t+1}(n)| \rangle$, which is how far (on average) from its current position the leader will be in the *next* wave front. The resulting distributions $\langle P(\Delta n) \rangle$ of these *jumps* are plotted in Fig. 3(A) for all system sizes. The largest probability corresponds to the case in which the wave front is first triggered from the same element as in the previous event. The power law n^{π} tells us that there is always a nonzero probability for a very long jump,

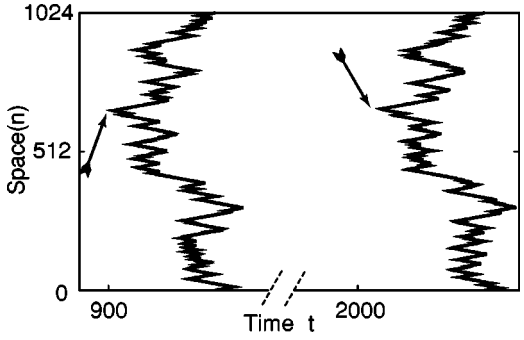

FIG. 1. An example of two consecutive noise-induced wave fronts. Note the similarity in the overall shape of the two consecutive wave fronts, which is typical. The arrows indicate the earliest activated site [i.e., the leader $L(n)$] in each wave front.

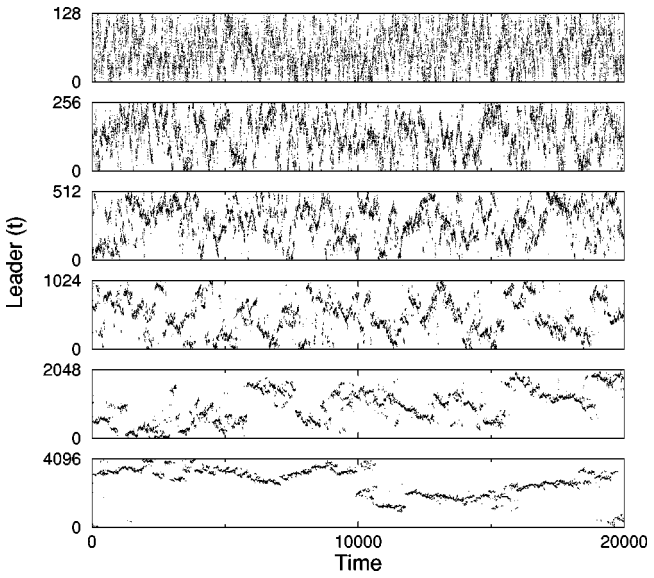

FIG. 2. Plot of the consecutive positions of the leading element in each firing event (i.e., the ones identified by the arrows in Fig. 1). The tendency of the leader is to remain near the previous leading site, a fact that is visually more apparent in the large systems. (The system size increases from $N=128$ at the top panel to $N=4096$ at the bottom panel. $\rho=10^{-2}$ for all panels.)

indeed as large as the entire system. Therefore, the cutoff of the power law is the only difference between the results obtained with small or large N [see panel (A) in Fig. 3].

Another related measure is the estimation of the average distance the leader drifts from its current position as a function of time lag Δt (t is always given in wave front's units). The results are plotted in panel (B) of Fig. 3. The fact that the log-log plot of $|\Delta n|$ vs Δt is linear implies a power law $\sim \Delta t^H$. The best-fit line of the results in Fig. 3(B) gives an exponent $H=0.19$. For this case it is known that the power spectrum decays as $1/f^{\beta}$, and that β relates with H as $\beta=2H+1=1.4$ (a random walk will have similar statistical behavior, but with an exponent $H=1/2$). These power laws, with cutoffs given only by the system size, imply a lack of characteristic scale (both in time and space), a situation which resembles some of the scenarios described in the context of self-organized criticality [7].

What causes this memory is trivially simple: the first site to be activated by the noise will necessarily be the first (exactly after r time steps) to be recovered and consequently to be ready to be re-excited. The two adjacent sites which were excited by the leader will recover only after $r+1$ time steps, and so on for the other adjacent sites. Thus excitation by the noise will always be biased by the previous sequence of excitation. Therefore, this ''memory'' can be preserved as long as the cycle of recovery (in this model the r time steps) is not affected by the noise. Regarding the dependence with the noise intensity, for vanishingly small ρ all sites will have enough time to cycle to the Q state, and no memory will be kept (see below).

Exponents are robust: The phenomenology and its power laws are not model dependent. We obtained similar results with various numerical models, so we sought the simplest numerical simulation scheme, which is a simple kinematic description of the motion of these noise-induced propagated excitable waves in the limit of infinite system size and low noise amplitude. The algorithm is as follows (see the cartoon in Fig. 4). Time and space are considered continuous variables. Excitations can initiate a wave front at any point, so the first step of the algorithm then is to distribute all potential excitation spots at random locations and times, as a two-dimensional (2D) Poisson process in x-t space with a probability $\rho(x,t)$ which we will take to be constant for now. Filled circles in Fig. 4 denoted a through e correspond to some of these events. The algorithm scan the space searching for the *earliest* excitation point (i.e., in the figure is the point a). Two wave fronts come forth from that point with unit speed. A front dies when it either reaches the boundary (as in the initial case in the figure) or upon colliding with other fronts as the one initiated by event labeled b (the dotted lines indicate two of these interrupted fronts). So, after locating the earliest point a, all other points satisfying $\Delta t > |\Delta x|$ (i.e. laying inside the space-time cone with vertex in a) are guaranteed to be ''ahead'' of point a. We now proceed to look for the earliest points which are *not* ahead of a (i.e., are outside the cone) until all other points are ahead of our cur-

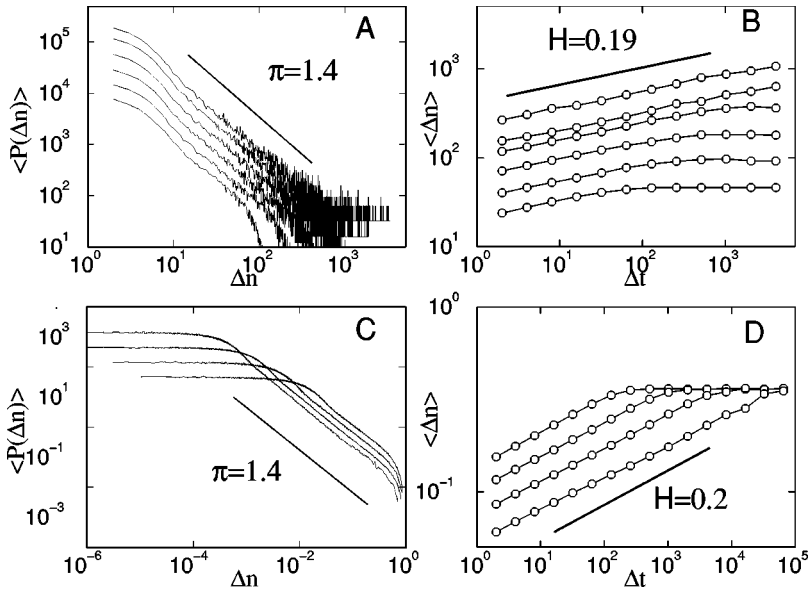

FIG. 3. [(A) and (C)] Distribution of the differences between $L(n)$ of two consecutive wave fronts. Results in (A) correspond to the discrete model, while results plotted in (C) are from the kinematic simulation. In both cases the exponent $\pi\sim 1.4$. [(B) and (D)] Mean drift of $L(n)$ as a function of time lag Δt. Results in (B) are from the discrete model, and those plotted in (D) are from the kinematic simulation. The mean drift scales as t^H, the best-fit line gives $H=0.19$ in the case of the discrete model, and $H=0.2$ for the results using the kinematic description. The system sizes for the discrete model are $N=128$, 256, 512, 1024, 2048, and 4096 from bottom to top plots, and the noise $\rho=10^{-2}$. For the kinematical description the system size is fixed (unit interval), and the noise density $\rho(x,t)$ increases from bottom to top—as determined by the steep part of the plots—from 10^{-6}, 10^{-5}, 10^{-4}, and 10^{-3}.

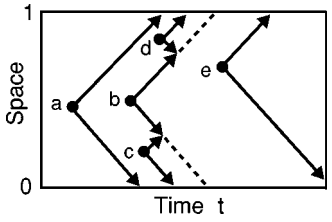

FIG. 4. Cartoon of the kinematic algorithm (see text).

rent collection. Using relativity terms, we scan the Poisson process for the largest collection of mutually spacelike points containing *a*, then locate the ''earliest'' point (in our reference frame) and repeat iteratively, as in a convex hull algorithm on Minkowski metrics. The results of such simulations are plotted in Fig. 3 alongside of those described for the discrete model. Jump distributions are plotted for four noise levels in panel (C). The mean drifts as a function of time lag are plotted in panel (D). It can be seen that there is a remarkable agreement between the numerical values of both scaling exponents. It needs to be noted that the kinematic algorithm used here is equivalent [10] to the polynuclear growth (PNG) model [8] studied extensively in the context of 1D growth processes. It has been shown that at least in one dimension, the PNG asymptotic behavior belongs to the Kardar-Parisi-Zhang universality class [9].

How long does it remember? For the sake of demonstration, the dissipation of memory can be estimated by first imposing an initial activation sequence in the system (i.e., writing) and then calculating the Hamming distance between the initial and subsequent wave front separated by Δt. Using the discrete model we impose an arbitrary initial configuration of excitation, in this case the sinusoidal pattern plotted in the inset of panel (A) of Fig. 5. As time passes, the pattern deforms as shown by the snapshots at times 2, 5, 10, and 50 in the figure, which can be estimated by the Hamming distance defined as

$$\langle D(t)\rangle = \frac{1}{N}\sum_{n=1}^{N} |S_n^t - S_n^{t+\Delta t}|, \tag{1}$$

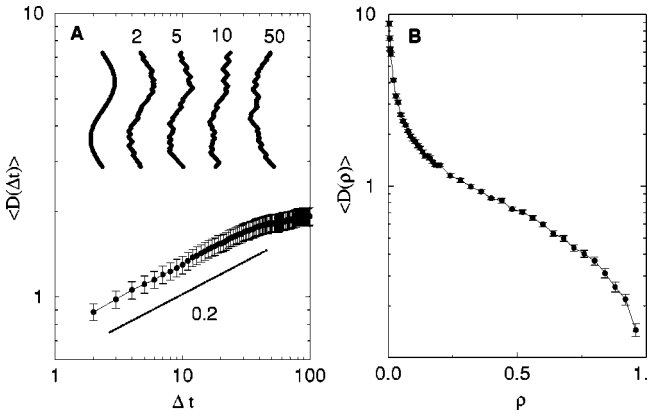

FIG. 5. (a) The Hamming distance $\langle D(t)\rangle$ from the original sinusoidal pattern as a function of time. The inset shows the initial wave front and at time steps: 2, 5, 10, and 50. $N=256$, $\rho=10^{-2}$ means, and SEM of 256 realizations. (b) The Hamming distance between two consecutive wave fronts is a monotonically decreasing function of noise ρ (means and SEM of 256 realizations).

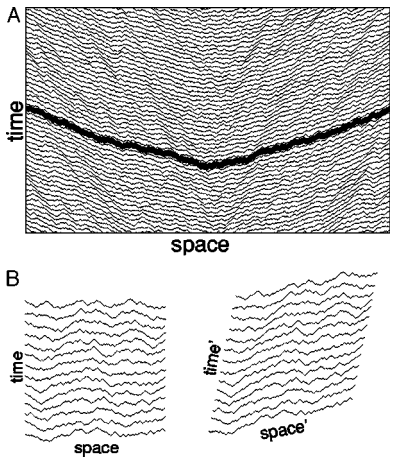

FIG. 6. (a) A spatial modulation of the noise density causes the fronts to be permanently pinned. Shown is the kinematic model, where the density of points has a cosinusoidal modulation on the *x* axis of 10%. Except for the darkened ones, only one out of ten fronts is shown. (b) Fronts are invariant under a Lorentz transform.

where *S* are the initial and subsequent states, ranked by the excitation order of each element. Means and standard error of the mean (SEM) $D(t)$ were calculated, and the results are plotted in the main body of Fig. 5(a) as a function of time. It can be seen that the Hamming distance follows a power law up to times of about 50 events. It was already mentioned that for vanishingly small ρ no memory of previous states can be maintained, since this condition implies that all the elements have enough time to go to the *Q* state preceding the excitation. Thus, rather paradoxically, more noise implies a longer memory. This is illustrated by the results in Fig. 5(b), where $D(t)$ was calculated for increasing noise ρ. Thus we call this phenomenon a form of *noise-induced memory*.

Inhomogeneities: It is important to address the effect of parameter fluctuations, since in any real system these values will not be constant in space or time. The same features endowing our system with a ''memory'' help to understand its sensitivity to variations in the parameters. For instance, a spatially varying noise level will result in the fronts being effectively pinned at the location of maximum noise strength; as shown in Fig. 6(a), a variation of only 10% in noise density can give rise to complete localization of the front. This feature can be understood readily within the kinematic model, if we note that the fronts, which represent waves of constant speed, are invariant under Lorentz transforms, as depicted in panel (b) of Fig. 6. Furthermore, the homogeneous Poisson point process used in the kinematic model is also invariant under Lorentz transformations. Think of the way the ''average'' layer of Fig. 6(b) looks: its average spacing Δt, average tilt $\langle dt/dx\rangle$, and point density ρ are related by $1/\Delta t=\sqrt{2\rho}\cosh\theta$, where θ is the parameter to the Lorentz transform; then $\langle dt/dx\rangle=\tanh\theta$. Looking back to Fig. 6(A), these relations hold as long as the mean separation between adjacent points in the Poisson process is smaller than the variations in ρ. Since Fig. 6(a) has to satisfy a constant average Δt independently of the point process density, we obtain $\sqrt{2\rho}\cosh\theta=\sqrt{2\rho_{\max}}$, where $\rho_{\max}$ is the maximum of $\rho(x)$; this implies that

$$\langle dt/dx \rangle = \sqrt{1 - \frac{\rho}{\rho_{\max}}}.$$

Implications for learning and memory: The dynamics described here might have important consequences for neural ''plasticity.'' This is the name given, in neuroscience, to the process by which interconnected neurons can strengthen or weaken their synaptic contacts to modulate their communication. The dogma is that memory and learning in animal brains are based on long-term changes of that synaptic connectivity. An important point in contemporary thinking assumes that whatever the plastic process is, it must be able to modify the synaptic strength during a time window given by the longest time scale in the neuron dynamics. This window is given by the relaxation kinetics of the membrane, and is at most of the order of hundreds of milliseconds [11], a length which is considered too short for producing most of the necessary synaptic changes. Our results can solve this discrepancy, since we have shown that the correlated activity lasts orders of magnitude more than the longest time scale of the model (i.e., the value of r). Thus the implication for real neurons will be that the spatial activity along the dendrites established by a given synaptic input will remain correlated for hundreds of firing events after the particular event. In other words, the neuron can in this way remember the location of the events that caused a firing. This correlated sequence of activation can in turn influence the spatial distribution of the molecular machinery supposedly responsible for the long-term synaptic modification necessary to remember.

The work reported here is restricted, for simplicity, to the one-dimensional case and the use of the simplest conceivable excitable model. Nevertheless, the phenomenon is shown to be robust, and similar results can be easily obtained using more detailed models. If the dynamic described here exist as such in real neurons, it would be very relevant to neural functioning.

This work was supported in part by the Sloan Foundation and the Norman & Rosita Winston Foundation. R.U. Computer resources are supported by NSF ARI Grants. Discussions with P. Bak, Maya Paczuski, R. Llinas, and Mark Millonas are appreciated. Communicated in part by DRC at the *First International Conference on Stochastic Resonance in Biological Systems, Arcidosso, Italy, May 5–9, 1998*, where the hospitality of the colleagues of the Istituto di Biofisica of Pisa was cherished.

[1] The literature on active channels is gargantuan; a recent survey can be found in Z. F. Mainen and T. J. Sejnowski, in *Methods in Neuronal Modeling*, 2nd ed., edited by C. Koch and I. Segev (MIT Press, Cambridge, MA, 1998), pp. 171–210.

[2] H. C. Tuckwell, *Stochastic Processes in the Neurosciences* (SIAM, Philadelphia, 1989).

[3] S. Kadar, J. Wang, and K. Showalter, Nature (London) **391**, 770 (1998).

[4] J. M. Greenberg and S. P. Hastings, SIAM (Soc. Ind. Appl. Math.) J. Appl. Math. **34**, 515 (1978).

[5] Other numerical formulations, including an explicit integrate and fire scheme, give similar results.

[6] By considering that in these systems the time to excite the whole system is smaller than the recovery time, we could safely assume $r > N$.

[7] P. Bak, C. Tang, and K. Wiesenfeld, Phys. Rev. Lett. **59**, 381 (1987); Phys. Rev. A **38**, 364 (1988); P. Bak, *How Nature Works: the Science of Self-Organized Criticality*. (Springer, New York, 1996); M. Paczuski, S. Maslov, and P. Bak, Phys. Rev. E **53**, 414 (1996).

[8] E. Ben-Naim, A. R. Bishop, I. Daruka, and P. L. Krapivsky, J. Phys. A **31**, 5001 (1998).

[9] M. Kardar, G. Parisi, and Y.-Z. Zhang, Phys. Rev. Lett. **56**, 889 (1986).

[10] We thank Hugues Chate (Saclay) for pointing out the potentially very fruitful connection between the PNG and excitable models.

[11] Basically one has to consider the decay to equilibrium of the membrane potential after being perturbed by the synaptic current. A rough figure of hundreds of milliseconds is the current estimate.